WCTE 2020
WORLD CONFERENCE ON TIMBER ENGINEERING
SANTIAGO, CHILE | 24 - 27 AUGUST

CYCLONE VULNERABILITY OF TRADITIONAL TIMBER HOUSING IN COASTAL REGIONS OF MADAGASCAR

Amanda C. Kaas[1], Yuner Huang[2], Chris T. S. Beckett[2], Alexandre S. Gagnon[3], Massimo A. Bollasina[2], Harinaivo Ramanantoanina[5], Holly A. Foster[2], Sarah M. McKee[2], Thomas P. S. Reynolds[2]

ABSTRACT: Madagascar is amongst the most vulnerable countries in the world to natural disasters. It is exposed to frequent cyclones and large proportions of its building stock collapse under the associated high wind loads and flood events. In the coastal regions of the country, domestic construction is based on timber, with infill walls and roofing made of eucalyptus, bamboo and traveller's palm. Carpentry connections such as pegged mortise and tenon joints are formed between timber members and are a key part of the load paths through the structure. This study takes a structural analysis of the timber structure and experimental testing of materials and components, and pairs it with analysis of the wind loads. In the framework we propose, the statistical variation of various parameters is included, allowing an estimate of the risk to a population of buildings in a given year: information which can be used to justify and target investments to improve resilience.

KEYWORDS: Carpentry connections, traditional construction, wind load, hardwood, cyclone resistance

1 INTRODUCTION

Cyclones cause extensive damage and loss of life in Madagascar. In March 2017, for instance, cyclone Enawo caused at least 81 deaths, destroyed 38,000 houses, and left 250,000 people displaced [1]. Traditional houses in the coastal region of Madagascar are based on timber. The purpose of this study was to demonstrate a framework for combining a simple structural analysis of a representative building, based on experimentally measured properties of materials and components, with statistical information on cyclone wind speeds, to assess its annual risk of failure.

NGOs such as Care International work with communities in Madagascar to help people improve the resistance of their homes to cyclones. The NGOs attempt improvements based on sound engineering principles, as shown in Figure 1 below, but they aren't currently able to quantify the risk to structures before and after these improvements, or to prioritise improvements based on those which have the greatest benefit.

This research seeks to address those shortcomings by developing a framework including a weakest-link analysis of the timber structural system and wind loads estimated from climate modelling, which can be used in any setting exposed to cyclones. By comparing the structural resistance of a population of buildings with a range of potential wind speeds, an estimated figure representing the number of houses failing in that population can be achieved. This is particularly useful to estimate the potential damage that a specific cyclone category may cause.

[1] Amanda C. Kaas, David Narro Associates, Edinburgh akaas@davidnarro.co.uk

[2] Thomas P. S. Reynolds, Institute for Infrastructure and Environment, School of Engineering, University of Edinburgh, UK t.reynolds@ed.ac.uk
Yuner Huang, Institute for Infrastructure and Environment, School of Engineering, University of Edinburgh, UK yuner.huang@ed.ac.uk
Chris T. S. Beckett, Institute for Infrastructure and Environment, School of Engineering, University of Edinburgh, UK Christopher.Beckett@ed.ac.uk
Holly A. Foster, Institute for Infrastructure and Environment, School of Engineering, University of Edinburgh, UK
Sarah M. McKee, Institute for Infrastructure and Environment, School of Engineering, University of Edinburgh, UK

[3] Alexandre S. Gagnon, School of Biological and Environmental Sciences. Liverpool John Moores University, UK. a.gagnon@ljmu.ac.uk

[4] Massimo A. Bollasina, School of GeoSciences, University of Edinburgh, UK Massimo.Bollasina@ed.ac.uk

[5] Ramanantoanina, Ecoles Superiéures U-Magis, Madagascar rilaidama@yahoo.co.uk

Figure 1: *Coastal house with improved features built by Care International showing key "Build back better" features.*

2 MATERIALS AND STRUCTURAL SYSTEM

Several species of timber are used in the construction of these houses, sourced from very near the site depending on what is readily available. These include extremely high-density tropical hardwoods such as Rosewood and Ebony. These species are now protected, and NGOs working to improve the resilience of these buildings base their designs around non-native Eucalyptus, which is potentially plantation-grown.

Figure 2: Schematic diagram of the structure showing the actions on it due to a cyclone, and some key points in the load path for analysis illustrates the basic structural form of a traditional house. The structure is founded on posts embedded into the ground. In some cases, these shallow 'piles' provide the only lateral load resistance. The timber members are connected using carpentry joints: pegged mortise and tenon connections, joining columns and beams at the elevated floor level, mid-height, and eaves level. The timber member at mid-height is not considered part of the primary structure but is used as a support for the cladding spanning between the floor and eaves. These members tend to have smaller diameters, as they experience lower loads at a shorter span.

Using experimental data linked to theoretical calculations, the likely weakest links were identified in the structural system. This allows a simplified analysis of the failure load for this type of structure.

Figure 2: Schematic diagram of the structure showing the actions on it due to a cyclone, and some key points in the load path for analysis shows the key parts of the structure which were considered in the analysis of its resistance to cyclone winds: the "short-pile" foundation, bending of the column and beam members, the connections within the frame and the roof-to-rafter connections. The green indicates primary members (70x70mm square sections) and the blue secondary members (50mm diameter).

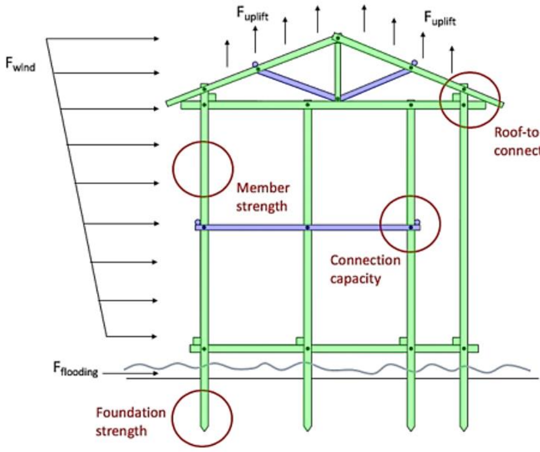

Figure 2: *Schematic diagram of the structure showing the actions on it due to a cyclone, and some key points in the load path for analysis*

The resistance of the traveller's palm, often used as cladding, was also evaluated to estimate potential increases in internal pressures, resulting in the roof blowing off - a failure often observed during cyclones. The roof consists of palm leaves tied to the rafters, providing the building with weather tightness.

3 EXPERIMENTAL METHODS

3.1 TIMBER PARAMETERS

Eucalyptus was selected for this study, based on the materials used on site. Due to the limited volume of material available, tests on eucalyptus followed standards for small clear specimens of timber [2]. This allowed a direct comparison with results in the literature for mechanical properties of Eucalyptus and other tropical hardwoods [3,4]. These generally follow either British or Australian standards for testing small-clear specimens, where 20x20x300mm specimens, with no visible knots, are cut from a piece of timber.

The experimental set-up is shown in Figure 3. The supports are spaced at 280mm centres with the load applied at midspan on the radial face of the specimen.

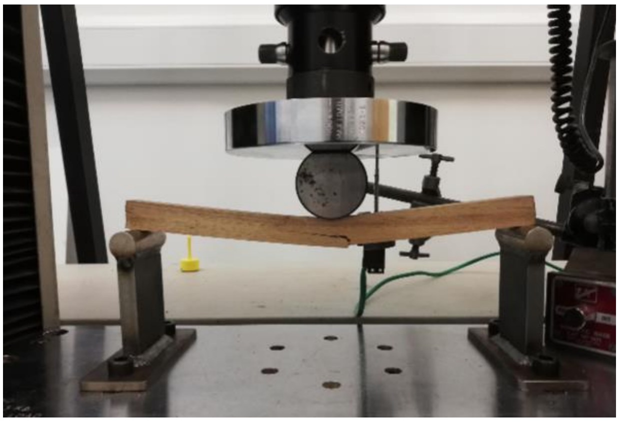

Figure 3: *Experimental set-up showing failure*

3.2 SOIL PARAMETERS

The angle of repose of the oven-dried sandy soil sample was tested using the set-up shown in Figure 4. A glass plate was used for an even surface with the funnel opening placed 25cm above, in accordance with Selig [3]. This method provides an initial estimate for the soil friction angle at shallow depths (i.e. with little soil confinement), as might be present at the depths of the foundations. In situ testing will be performed to determine the soil density; in the interim, a dry unit weight of 18 kN/m^3 was assumed, as a typical value for sandy soils at a medium density.

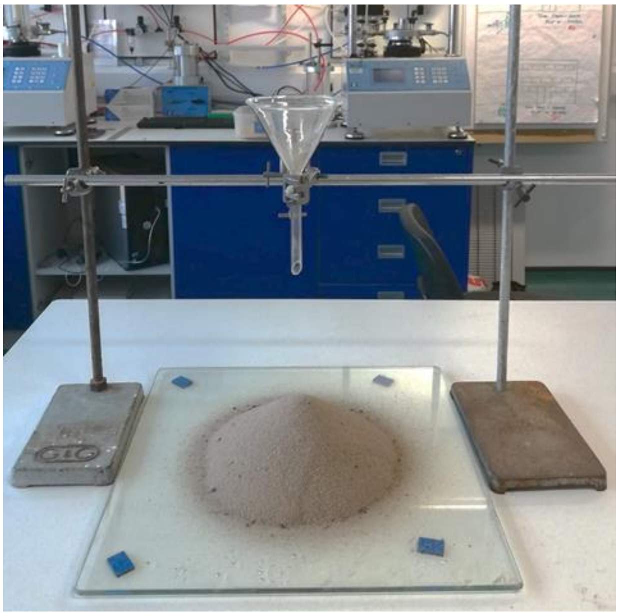

Figure 4: *Experimental set-up for soil testing*

4 METHODS OF ANALYSIS

4.1 CLIMATE MODEL DATA

Mean monthly wind speeds at 10m height from the ERA5 dataset [4] during the period 1979-2000 were compared to in-situ observations as recorded at the Météo Madagascar [5] weather station at Antalaha for the same time-period. The monthly average wind speed data show that the ERA5 data follow the seasonality of the measured data well, but with an inherent underestimate (Figure 5).

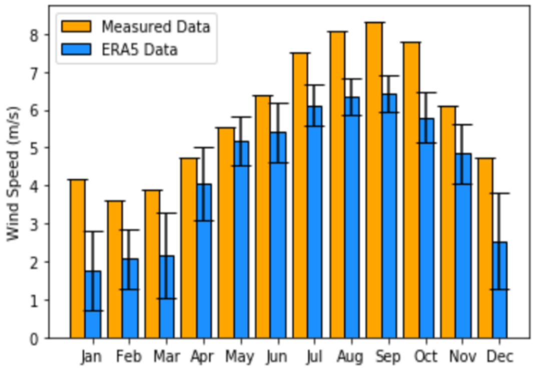

Figure 5: *Comparison of monthly average wind speeds between Antalaha weather station and the corresponding grid cell in ERA5*

Instantaneous wind gusts at a 10m height were extracted from the ERA5 dataset for the grid cell corresponding to Antalaha for the period 1979-2014. For each year, the annual maximum wind gust was identified and then converted to 10-minute mean wind speeds [6] for use with Eurocode 1 [7]. The Eurocode calculations are based on the 10-minute mean wind velocity for a return period of 50 years. As the 10-minute wind speeds are not a direct output of ERA5, the 3s instantaneous wind gust was extracted from ERA5 and converted to the 10-minute mean wind speed using the World Meteorological Organisation guidelines for converting between various wind averaging periods during cyclonic conditions.

The annual maxima showed two separate classes of wind speeds, which were taken to correspond to years in which cyclone winds affected that location (n=3) and years without cyclone winds at that location (n=33). These data were well fitted by two separate Extreme Value Type I (Gumbel) distributions, as shown in Figure 6.

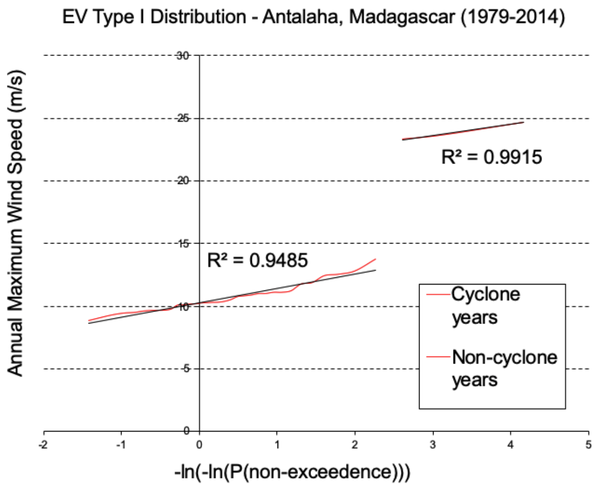

Figure 6: *Fitting Gumbel distributions separately to cyclone years and non-cyclone years.*

4.2 RELATIONSHIP TO PRESSURE ON THE BUILDING ENVELOPE

The pressure on the building envelope w_e was related to the 10-minute mean wind speed taken from the ERA5 dataset, equivalent in this case to v_b by Equation (1), based on Eurocode 1 Part 1-4 [7].

$$w_e = C_e(z) * \left[\frac{1}{2}\rho v_b^2\right] * C_{pe} \tag{1}$$

where, $C_e(z) = 2.5$ and $\rho = 1.225$ kg/m^3. C_{pe} is the pressure coefficient for the particular part of the building envelope and is evaluated for each element being considered.

4.3 TIMBER CONNECTIONS

The strength of carpentry joints was based on the geometry, experimental bending strength and density of the peg and surrounding material. Shanks et al. [8] show that the European Yield Model presented in Eurocode 5 [9] can be used to estimate the strength of all-timber pegged connections.

It should be noted that the strength of members used in the present example does not consider the effects of potential elevated moisture content, which is likely to be important in a tropical climate, and under the extreme rainfall associated with cyclones.

There is no generic size of peg used in all carpentry joints across Malagasy buildings. An example of a pegged mortise and tenon connection used locally is shown in Figure 7 and shows that these are hand-crafted and likely to vary in both size and cross-section shape.

Figure 7: *Example of traditional pegged mortise and tenon connection (image from Care International)*

4.4 FOUNDATION ANALYSIS

The house comprises of a shallow foundation formed from 40 square 70×70 mm posts driven into the ground at irregular intervals. Several methods were examined to assess this type of 'informal' foundation, namely considering the foundation to be: i) a continuous shallow slab foundation; ii) group of short piles; iii) a group of embedded stakes. Of these approaches, (i) resulted in a significant overestimation of the likely capacity, given that the soil within the foundation's perimeter was considered also to act as part of the footing. This approach was therefore discounted and will not be reported here.

Eurocode 7 (BS EN 1997-1:2004, incorporating the UK National Annex in the absence of equivalent guidance for Madagascar) was used to analyse the performance of the embedded posts as short piles, following methods described in [10]. It should be noted, however, that these methods were not developed with such short piles in mind, whereby the majority of the soil fails in an unconfined manner (as opposed to larger piles, whose greater depth increases the soil confinement and permits the soil to fail plastically). Results from approach (ii) were therefore compared to approach (iii), following design guidance for wooden staked anchors given in [11] and where the tensile capacity of the stakes was assumed to equal 80% of their compressive capacity [12]. Results for approach (iii) marginally exceeded those found for approach (ii), indicating that approach (ii) was sufficiently suitable for use in shallow soils. Approach (ii) was therefore adopted to estimate the foundation capacity.

All calculations were completed assuming a water table at the surface, demonstrated to be the worst-case scenario for vertical bearing capacity and representative of flooding during a cyclone, for a drained soil condition. Given that the soil is sandy, the pile group efficiency was assumed to equal unity, i.e. the pile group was unable to mobilise additional capacity due to any soil trapped within the group perimeter. The soil-structure friction angle δ was assumed to equal 25° and the soil pressure coefficient

K to equal 1.5, representing soil stresses around a driven pile.

Horizontal capacities were not assessed as part of this work but will be examined in future studies. Furthermore, additional vertical loading arising from the horizontal (moment) wind loading was not considered, as the flexibility of the structure (a function of the connection resistances) is unknown. Such additional loading will also be considered in future analyses.

4.5 FIRST ORDER RELIABILITY METHOD

The wind speeds were shown to reasonably follow a Gumbel (EV Type I) distribution and the force applied to an element is proportional to the velocity squared, which leads to a nonlinear limit state function. The First Order Reliability Method [13, 14] was therefore applied to estimate the failure probability for each element in a cyclone year, and in a non-cyclone year.

The failure probability due to cyclone winds was then calculated as the failure probability in a cyclone year multiplied by the probability of a cyclone occurring in a given year. Non-cyclone winds were assumed to occur every year, and so the failure probability due to non-cyclone winds is equal to the failure probability in a non-cyclone year.

The annual probabilities of survival due to cyclone or non-cyclone winds were then combined, as is done by Yeo, Lin and Simiu [15] to give a "mixed" probability of a particular wind speed being exceeded, in this case to give a "mixed" annual probability of survival through the below Equation (2):

$$p_{(survival)} = p(F_{nc} < F_{max})p(F_c < F_{max}) \qquad (2)$$

where the subscript c refers to cyclone and nc non-cyclone winds.

5 EXPERIMENTAL RESULTS

Eucalyptus timber was obtained from Madagascar, representative of that used in the primary and secondary structural members. This was used in mechanical testing, along with traveller's palm used for cladding. A soil sample was obtained from a coastal village in Madagascar.

5.1 MALAGASY EUCALYPTUS AND TRAVELLER'S PALM

The bending capacity of local eucalyptus was measured, as well as the traveller's palm used to infill the walls.

A total of 17 small clear specimens (20x20x300mm) of eucalyptus were tested, cut from two larger pieces imported from Madagascar. The variability in this sample was not expected to be a good indicator of variability across a population of buildings, but nonetheless provides a set of data with which to demonstrate the application of the proposed reliability analysis.

Figure 8 gives the force-displacement results obtained during testing. Although the specimens were stored in the same conditioning laboratory prior to testing, they still had substantially different moisture content at the time of testing. The two levels of moisture content (MC) proved to be an important factor influencing the bending behaviour. Specimens with approximately 20% MC responded to the loading in a more ductile manner (shown in red below), compared with the specimens with approximately 8% MC (shown in black below). The specimens at 8% moisture content had a higher mean strength but higher variation in strength than those at 20%.

This serves to highlight the potential influence of moisture content on the behaviour of the timber elements in these structures.

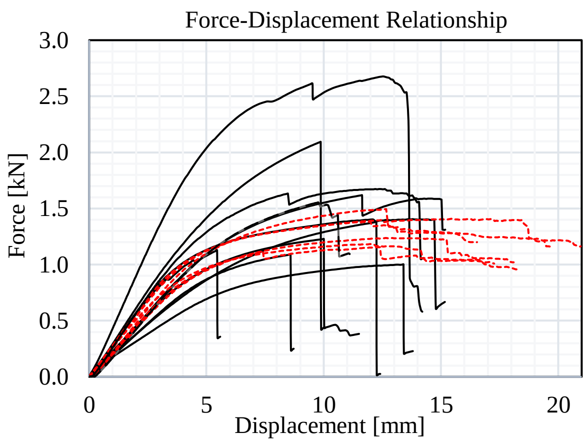

Figure 8: *Force-displacement relationship from small clear specimen experiments*

The modulus of rupture (MOR) was calculated for each specimen to evaluate the variation in strength of a full-sized member, using the peak load and corresponding deflection.

The mean MOR was 77.23 N/mm^2, with a standard deviation of 18.83 N/mm^2, providing a full-sized (70mm by 70mm) member strength of 7.67kN with a standard deviation of 1.87kN.

It was concluded that the variation in strength of the ductile specimen was very similar to that of 6-year old eucalyptus grown in Brazil [16], as shown in Figure 9 below.

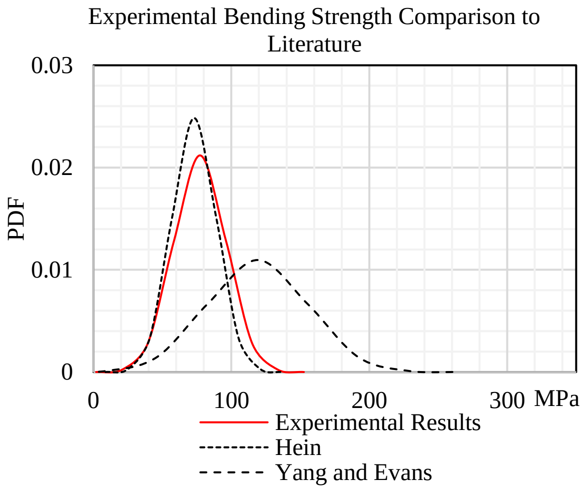

Figure 9: *Experimental results compared to Hein [16] and Yang & Evans' [17] results described in literature*

Hein [16] tested 230 specimens cut from 100 different 6-year old eucalyptus trees, with a mean circumference of 62cm and height of 23m. The variation in strength found by Yang and Evans [17] in Australia was much greater than that of Hein's [16] results. The specimens tested by Yang and Evans were from a plantation growing various eucalyptus species at ages ranging from 15 to 31 years old. The range in species and age provide a large variation strength [17].

Further experiments were carried out on eucalyptus samples with smaller diameters used at mid-height of the structure. These experiments used the same set-up as the small clear specimens, except that the full cross section (50mm diameter) of these members could be tested. From tests, the strength of a full-sized 0.55m long member was found to be 1.98kN with a standard deviation of 0.5kN.

Similarly, traveller's palm was tested in its full cross section over a 280mm span. For a full-sized member spanning 1.15m, the mean strength was estimated to be 0.05kN with a standard deviation of 0.004kN. As shown in Figure 1, the cladding uses many layers of traveller's palm, and an estimated number of 20 members per panel was therefore used to assess the panel strength. This strength was calculated based on a uniformly distributed wind load and does not include impact from airborne objects.

5.2 SOIL EXPERIMENTS

The angle of repose was found to be 24 degrees, with a moisture content prior to testing of 5% and a dry unit weight of 18kN/m^3.

6 STRUCTURAL RELIABILITY ANALYSIS

The load capacity of key elements in the structural system was assessed based on parameters from the characterisation of the local materials described in Section 0. These were then used along with the fitted distributions of annual maximum 10-minute wind speeds in the structural reliability analysis according to the First Order Reliability Method.

This gave an annual probability of failure corresponding to cyclone years and non-cyclone years. Table 1 summarises the probability of failure of each analysed member, and the combined probability of failure based on all of those.

Table 1: *Element failure probabilities*

Member	Probability of Failure (%)
Primary Members	0.02
Secondary Members	1.24
Cladding	6.9×10^{-6}
Roof-to-Rafter Connection	4.4×10^{-4}
Wall-to-Wall Connection	4.4×10^{-4}
Shallow Pile Foundation	4.6×10^{-5}
All the above causes	1.26

As described in Table 1, the members most likely to fail under the present assumptions about material and geometry are the secondary members. The probability of failure for those is 1.24%, equivalent to 1,240 houses expected to fail each year in a population of 100,000. It is expected that once the secondary members fail, the probability of failure of the cladding panels increases. If the cladding fails, the internal pressure magnifies, increasing the probability of failure of the roof-to-rafter connections. The above probabilities do not consider the effects of an object hitting the structure during high winds.

This method can be used to indicate the effectiveness of structural interventions to help reduce the rate of failure. The above can be demonstrated by investigating the change in likelihood of failure of the connections by changing the peg diameter. The above connection strength corresponds to a peg diameter of 25mm. The correlation between the annual number of failures in a population of 100,000 houses and the peg diameter is shown in Figure 10 below.

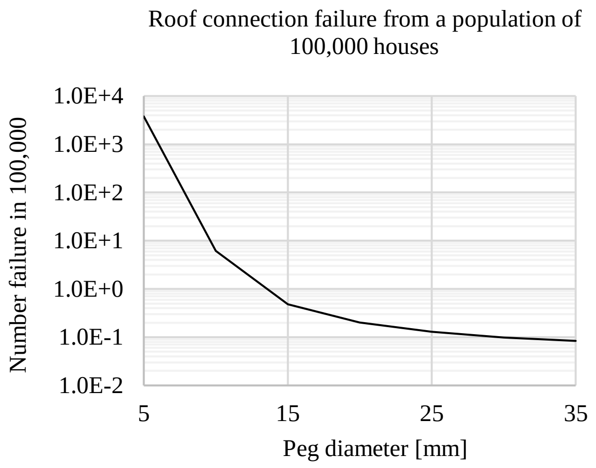

Figure 10: *Number of annual roof-to-rafter connection failures per 100,000 houses.*

Figure 10 is based on Shanks' [8] four failure modes for all-timber pegged connections. The mean and standard deviation of strength was estimated for each failure mode, and it should be noted that, since the coefficient of variation is different between modes, the mode with the lowest mean strength did not always give the highest probability of failure. Figure 10 shows the highest probability of failure for each peg diameter irrespective of the failure mode. Future analyses will combine the probabilities from every failure mode.

The coefficient of variation (COV) was assumed to be constant for all peg diameters in a given failure mode, and the COV derived from the results for the 25mm peg was used. Further work is required to investigate the statistical distribution of connection strengths.

As shown in Figure 10, the rate of failure reduces significantly by increasing the peg size, hence the use of a logarithmic scale. This approach has been used as a way of estimating the strength of the connections and corresponds with the non-linear failure mode expected to see. For higher accuracy, pegged mortise and tenon connections of various diameters should be tested on a large scale using Malagasy eucalyptus.

7 UNDERESTIMATE OF FAILURE PROBABILITY

The probability of failure estimated in this study is low and does not represent the observed failures of these dwellings under cyclone winds. We consider that there are two reasons for this: an underestimate of the variability of strength parameters and an underestimate of the wind speeds.

The variability of strength parameters will be underestimated because all the specimens tested were taken from a small volume of material from a single site in Madagascar. This will not accurately reflect the expected variation across a large population of buildings in different villages. The current project will include field tests of components constructed by local people across a number of sites, allowing a more accurate estimate of the true distribution of strength.

This analysis has shown that wind speed and inherently gust winds are underestimated. At the weather station of Antalaha, for instance, Météo Madagascar recorded the highest wind speed to be 60 m/s during the period 1971-2000, although this recorded maximum wind speed might not have been sustained over 10 minutes. Sustained wind speeds of approximately 57 m/s were also reached during cyclone Enawo in 2016, which made landfall in the North East of Madagascar near Antalaha but took place outside the 1979-2014 period that the current study focuses on. According to the ERA5 dataset, the 10m maximum gust wind recorded over the grid cell for Antalaha during the period 1979-2014 was 40 m/s, corresponding to a 10-minute mean wind speed of ~17.5 m/s.

Differences in wind speeds between ERA5 and the data from the corresponding weather station are nonetheless inevitable given that weather station data represent conditions at a specific point in space, while ERA5 represents wind speed data averaged over a grid cell, and cannot thus represent variability on spatial scales smaller than the grid. Moreover, wind conditions are affected by the local terrain and vegetation type for which the ECMWF Integrated Forecasting System that produces ERA5 can provide only an average value over an entire grid cell with a spatial resolution of 31km.

Figure 5 shows the underestimate in the monthly average wind speeds. As this project continues, we will work with Météo Madagascar to use the time series of weather station data at shorter averaging periods to give an accurate estimate of the expected wind speeds.

8 RESULTS AND CONCLUSIONS

With the analysis framework established, the risk to a population of houses can be calculated, resulting in a rate of failure of each component as shown in Figure 9, in this case measured as the number of annual failures per 100,000 houses.

As shown in Figure 10, parameters can be varied in the analysis to predict the effect of changing elements of the building construction, in this case the diameter of the peg used in the pegged mortise and tenon connections.

Further research and testing are ongoing to provide a robust set of input parameters, based on field surveys and experimental testing, which will allow this method to be used to make predictions of the true level of risk to this type of housing in Madagascar. This method of estimating failure can be a useful tool in preparing for cyclone response in LDCs.

ACKNOWLEDGEMENT

This research team was assembled under a Royal Academy of Engineering Frontiers of Engineering Development network, and research work has continued under a Royal Society Challenge-Led research grant. Thanks to Care International and the Catholic Relief Service for valuable insight into local construction practices and their proposals for improved cyclone-resistant construction.

REFERENCES

[1] P. Probst et al., 2017. *Tropical Cyclone ENAWO Post-Event Report*.

[2] BSI, BS373 (1957) Methods of testing small clear specimens of timber

[3] Selig, E.T., 1973. *Evaluation of relative density and its role in geotechnical projects involving cohesionless soils.* Journal of Materials in Civil Engineering, 21 (1).

[4] Hersbach, H. et al. (2020) 'The ERA5 global reanalysis', Quarterly Journal of the Royal Meteorological Society, 146(730), pp. 1999–2049. doi: 10.1002/qj.3803.

[5] Météo Madagascar: www.meteomadagascar.mg/ (direct communication)

[6] Harper, B. A., Kepert, J. D. and Ginger, J. D. (2010) *Guidelines for Converting Between Various Wind Averaging Periods in Tropical Cyclone Conditions WMO/TD-No. 1555*.

[7] CEN (2005) 'BS EN 1991-1-4:2005 Eurocode 1 Actions on structures. General actions. Wind actions.' BSI.

[8] Shanks, J. and Walker, P. (2009) 'Strength and Stiffness of All-Timber Pegged Connections', *Journal of Materials in Civil Engineering*. ASCE, 21(1), pp. 10–18

[9] CEN (2014) 'BS EN 1995 Eurocode 5: Design of timber structures - Part 1-1: General - Common rules and rules for buildings'. BSI.

[10] Fleming, K., Weltman, A., Randolph, M. & Elson, K. (2009). Piling Engineering. Taylor & Francis Group, London

[11] IFAI (2004). The IFAI procedural handbook for the safe installation and maintenance of tentage. Second Edition, Industrial Fabrics Association International

[12] De Nicola, A., Randolph. M., 1993. Tensile and compressive shaft capacity of piles in sand. Journal of Geotechnical Engineering, 119(12): 1952-1973

[13] CEN (2002) 'BS EN 1990:2002 +A1:2005 Eurocode 0 - Basis of Structural Design'. BSI.

[14] Kohler, J. et al. (2016) COST FP1401 Training School Materials

[15] Yeo, D., Lin, N. and Simiu, E. (2014) 'Estimation of hurricane wind speed probabilities: Application to New York city and other coastal locations', *Journal of Structural Engineering*, 140(6), pp. 6–10.

[16] Hein, P.R.G., Silva, J.R.M. and Brancheriau, L., 2013. *Correlations among microfibril angle, density, modulus of elasticity, modulus of rupture and shrinkage in 6-year-old Eucalyptus urophylla× E. grandis*. Maderas. Ciencia y tecnología.

[17] Yang, J.L. and Evans, R., 2003. *Prediction of MOE of eucalypt wood from microfibril angle and density.* Holz als Roh-und Werkstoff.